VBF Higgs Production at NLO QCD

Terrance Figy

IPPP

Durham University

Outline

VBF Higgs production at NLO QCD

- VBF Higgs + 2 jets at NLO QCD
- Anomalous Higgs Couplings
- MSSM VBF h(H) + 2 jets
- VBF Higgs + 3 jets at NLO QCD

Goals of Higgs Physics

- Discover the Higgs boson
- Measure its couplings and probe mass generation for gauge bosons and fermions

Fermion masses arise from Yukawa couplings via $\Phi^\dagger \to \left(0, \frac{v+H}{\sqrt{2}}\right)$

$$\mathcal{L}_{\text{Yukawa}} = -\Gamma_d^{ij}\bar{Q}_L'^i \Phi d_R'^j - \Gamma_d^{ij*}\bar{d}_R'^i \Phi^\dagger Q_L'^j + \ldots = -\Gamma_d^{ij}\frac{v+H}{\sqrt{2}}\bar{d}_L'^i d_R'^j + \ldots$$
$$= -\sum_f m_f \bar{f} f \left(1 + \frac{H}{v}\right) \quad (1)$$

- Test SM prediction: $\bar{f} f H$ Higgs coupling strength $= m_f/v$
- Observation of $H f \bar{f}$ Yukawa coupling is no proof that a v.e.v exists

Higgs coupling to gauge bosons

Kinetic energy term of the Higgs doublet field:

$$(D^\mu\Phi)^\dagger(D_\mu\Phi) = \frac{1}{2}\partial^\mu H\partial_\mu H + \left[\left(\frac{gv}{2}\right)^2 W^{\mu+}W^-_\mu + \frac{1}{2}\frac{(g^2+g'^2)v^2}{4}Z^\mu Z_\mu\right]\left(1+\frac{H}{v}\right)^2$$

- W,Z mass generation: $m_W^2 = \left(\frac{gv}{2}\right)^2, m_Z^2 = \frac{(g^2+g'^2)v^2}{4}$
- WWH and ZZH couplings are generated
- Higgs couples proportional to mass: coupling strength $= 2m_V^2/v \approx g^2 v$ within SM

Measurement of WWH and ZZH couplings is essential for identification of H as agent of symmetry breaking: Without a v.e.v such a trilinear coupling is impossible at tree level.

Total SM Higgs cross sections at the LHC

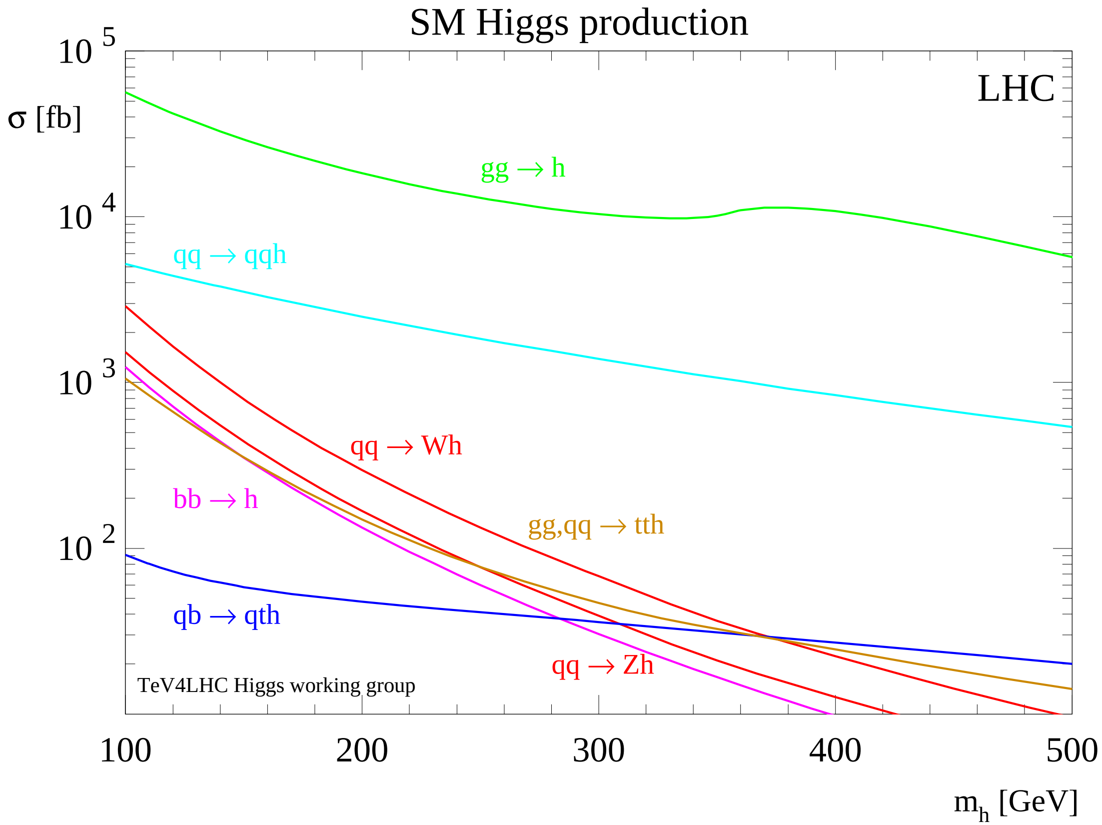

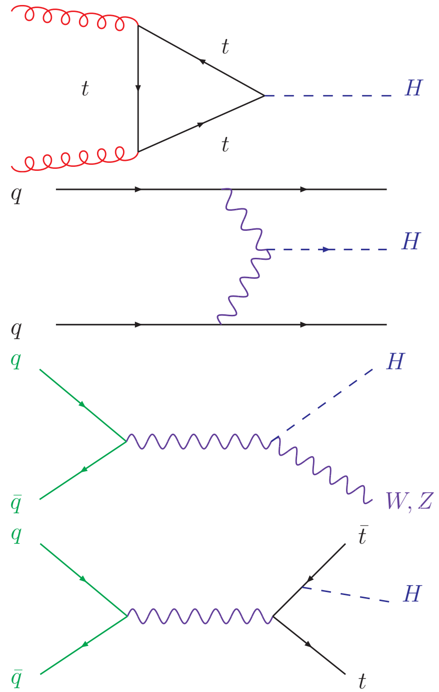

Decay of the SM Higgs

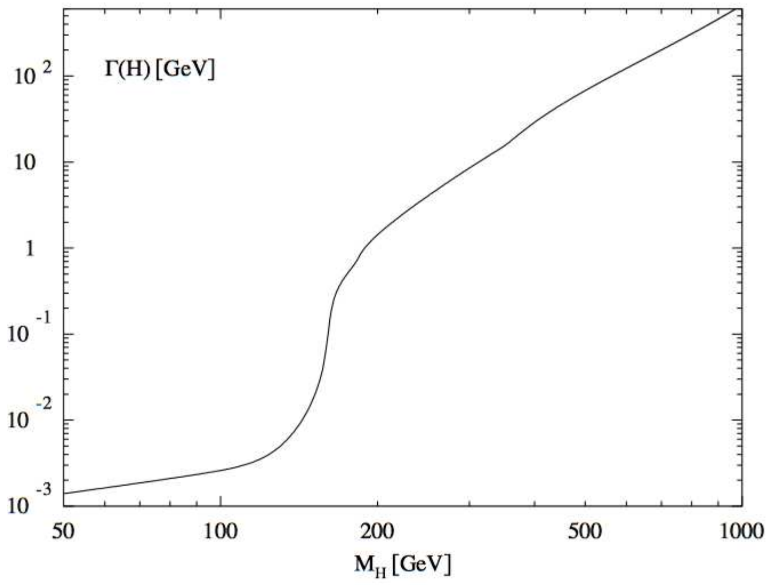

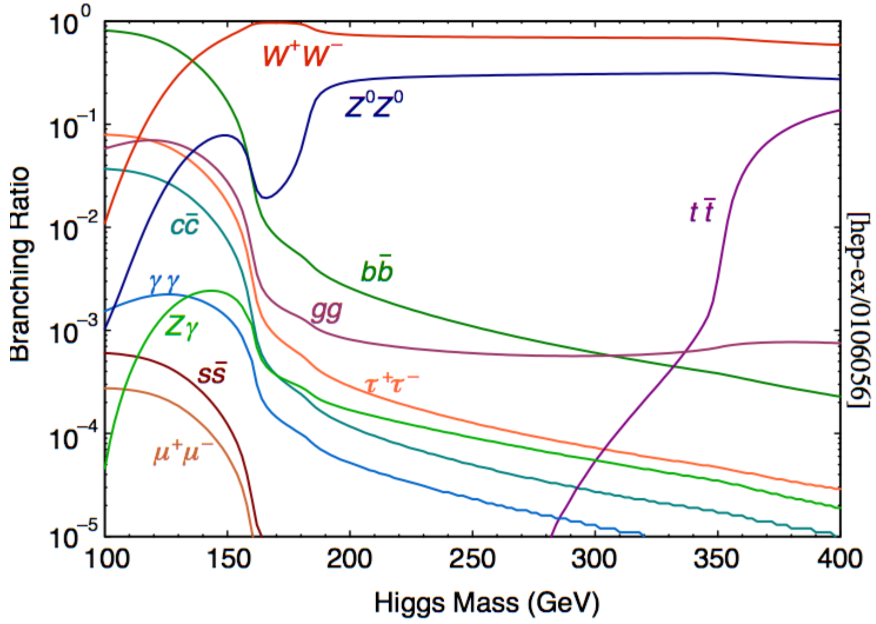

Vector Boson Fusion

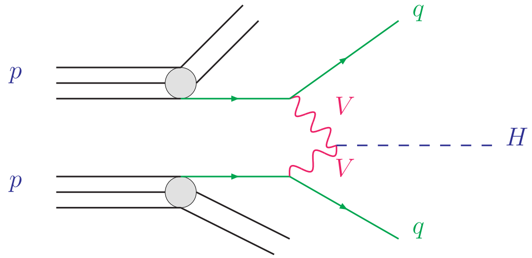

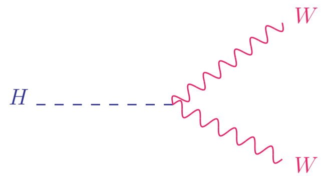

$m_H > 120$ GeV

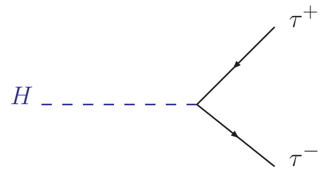

$m_H < 140$ GeV

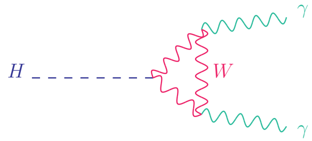

$m_H < 150$ GeV

[Eboli,Hagiwara,Kauer,Plehn,Rainwater,Zeppenfeld,. . .]

Most measurements can be performed at the LHC with statistical accuracies on the measured cross sections times branching ratios, $\sigma \times \mathrm{BR}$, of order 10% (sometimes even better).

Statistical and systematic errors at the LHC

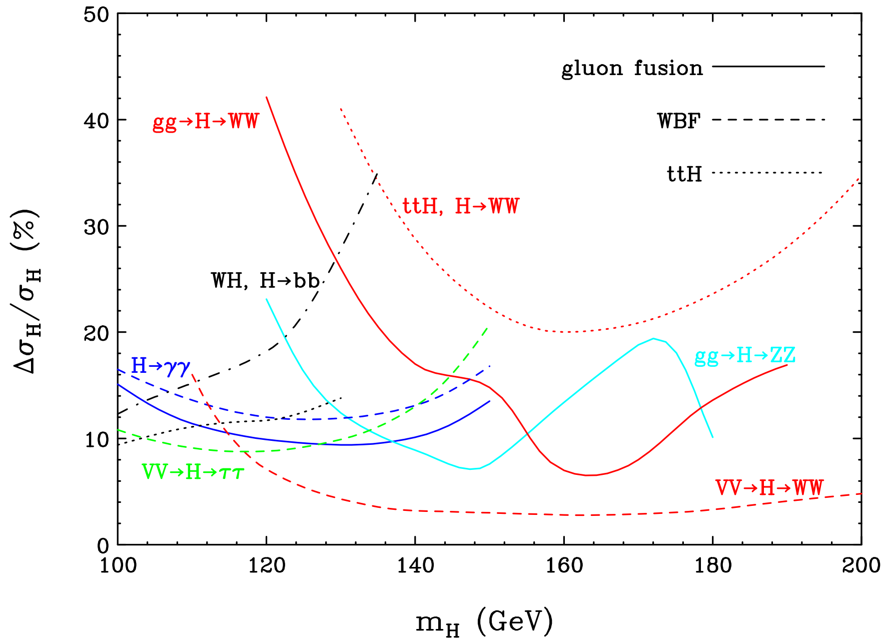

Assumed errors in fits to couplings:

- QCD/PDF uncertainties
  - ±5% for VBF
  - ±20% for gluon fusion
- luminosity/acceptance uncertainties
  - ±5%

VBF Signature

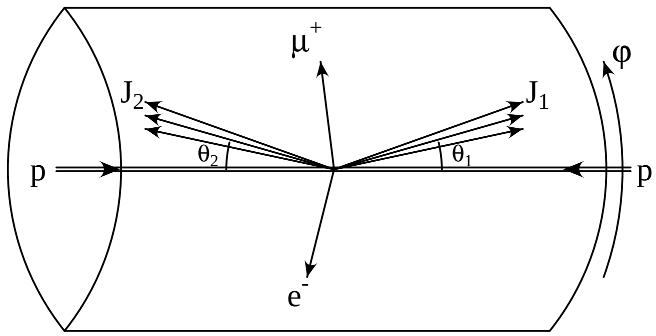

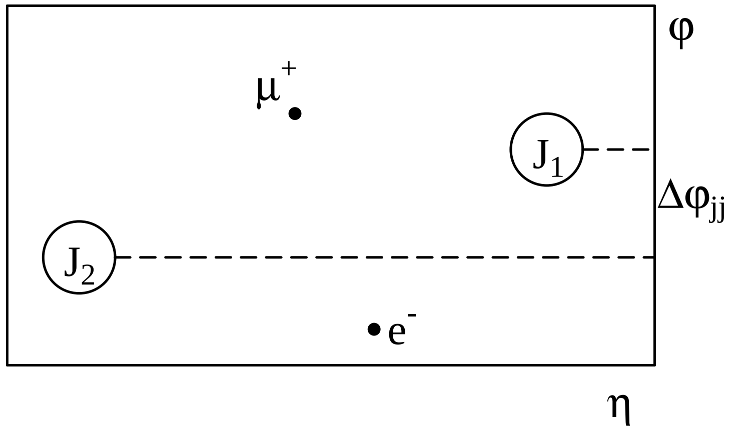

$$\eta = \frac{1}{2} \log \frac{1 + \cos\theta}{1 - \cos\theta}$$

- Energetic jets in the forward and backward directions ($p_T > 20$ GeV)
- Higgs decay products between tagging jets
- Little gluon radiation in the central-rapidity region, due to colorless W/Z exchange (central jet veto: no extra jets with $p_T > 20$ GeV and $|\eta| < 2.5$)

The NLO Calculation

Virtual Corrections

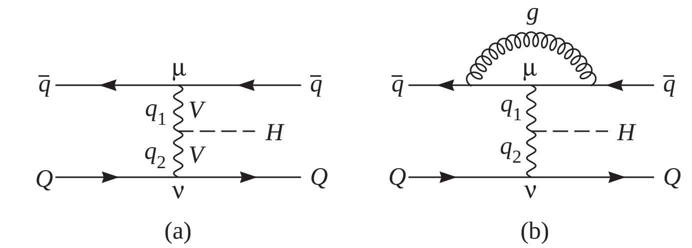

Real Corrections

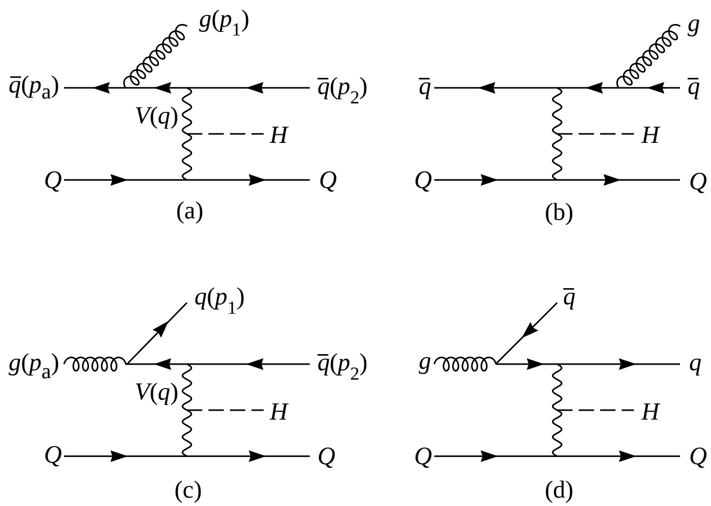

[T. Figy, C. Oleari and D. Zeppenfeld, Phys. Rev. D **68**, 073005 (2003)]

Applied Cuts

- Require two hard jets with $p_{Tj} \geq 20$ GeV, $|y_j| \leq 4.5$
- Higgs decay: $p_{T\ell} \geq 20$ GeV, $|\eta_\ell| \leq 2.5$, $\Delta R_{j\ell} \geq 0.6$
  Additionally, the Higgs decay products are required to fall between the tagging jets.

$$y_{j,min} < \eta_{\ell_{1,2}} < y_{j,max}$$

- Backgrounds to VBF are significantly suppressed by requiring a large rapidity separation of the two tagging jets.

$$\Delta y_{jj} = |y_{j_1} - y_{j_2}| > 4$$

Tagging Jet Selection

- p_T **-method**: Define the tagging jets at the two highest p_T jets in the event.
- E **-method**: Define the tagging jets as the two highest energy jets in the event.

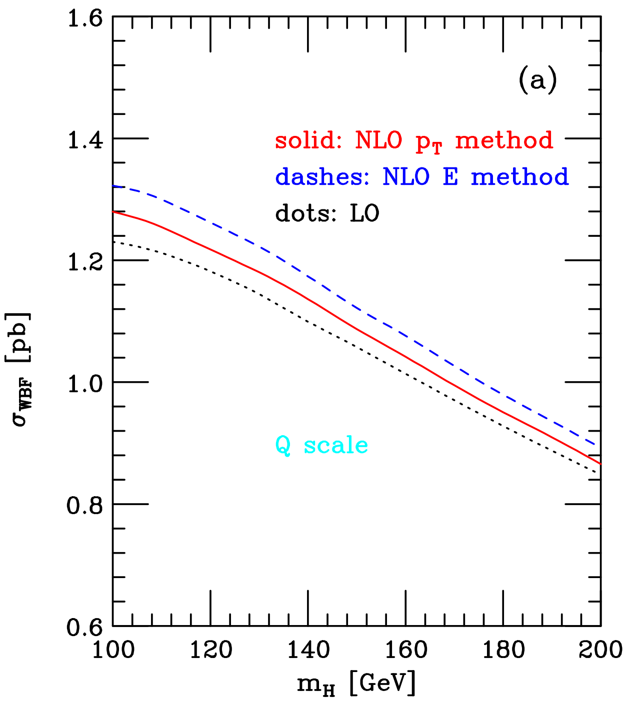

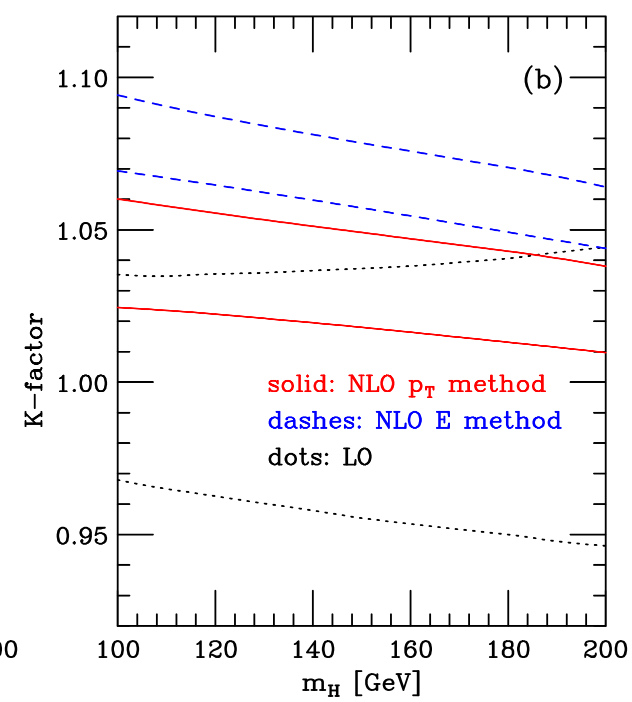

$$K = \frac{\sigma(\mu_R, \mu_F)}{\sigma^{LO}(\mu_F = Q_i)}$$

- p_T method: 3-5 % higher than LO
- E method: 6-9 % higher that LO

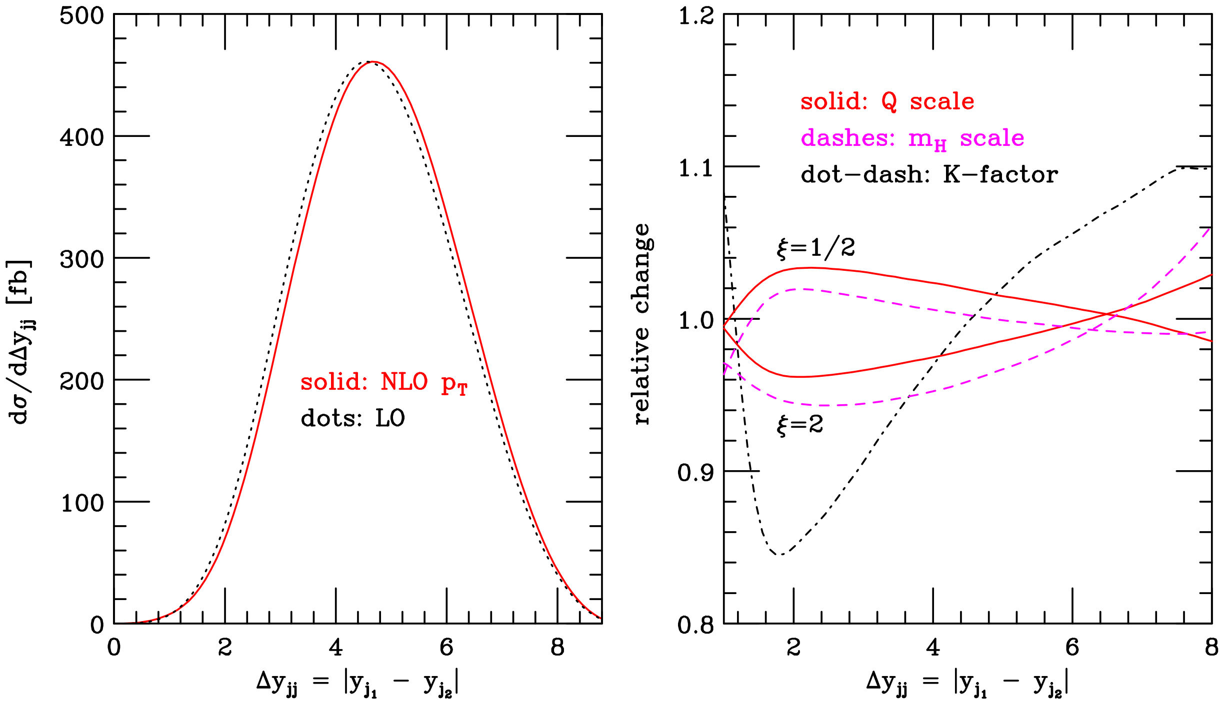

Tagging jets are slightly more forward at NLO than at LO

⇓

$\Delta y_{jj} > 4$ cut works well at NLO.

General Tensor Structure for the HVV vertex

$$T^{\mu\nu}(q_1, q_2) = a_1(q_1, q_2) g^{\mu\nu} + a_2(q_1, q_2)[q_1 \cdot q_2 g^{\mu\nu} - q_2^\mu q_1^\nu] + a_3(q_1, q_2)\varepsilon^{\mu\nu\rho\sigma} q_{1\rho} q_{2\sigma}$$

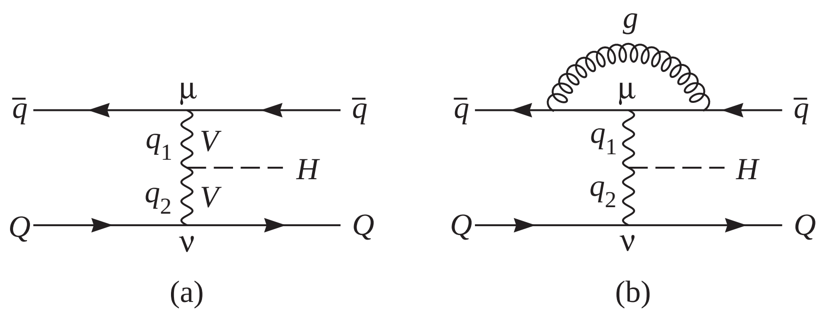

- SM-like: a_1
- CP even: a_2
- CP odd: a_3

The QCD corrections to Higgs production via VBF are computed in the presence of anomalous HVV couplings using VBFNLO. [a]

[a] T. Figy and D. Zeppenfeld, Phys. Lett. B **591**, 297 (2004)

p_{T_j} distributions

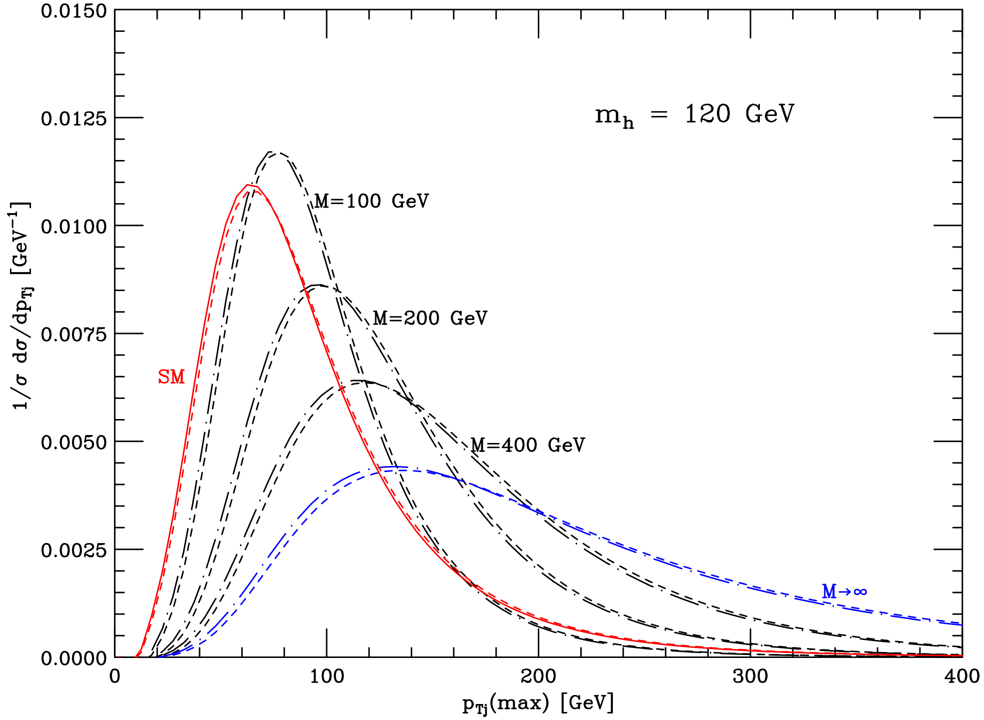

$$a_i(q_1, q_2) = a_i(0,0)\frac{M^2}{|q_1^2| + M^2}\frac{M^2}{|q_2^2| + M^2}$$

$\phi_{jj} = |\phi_{j_1} - \phi_{j_2}|$ distributions

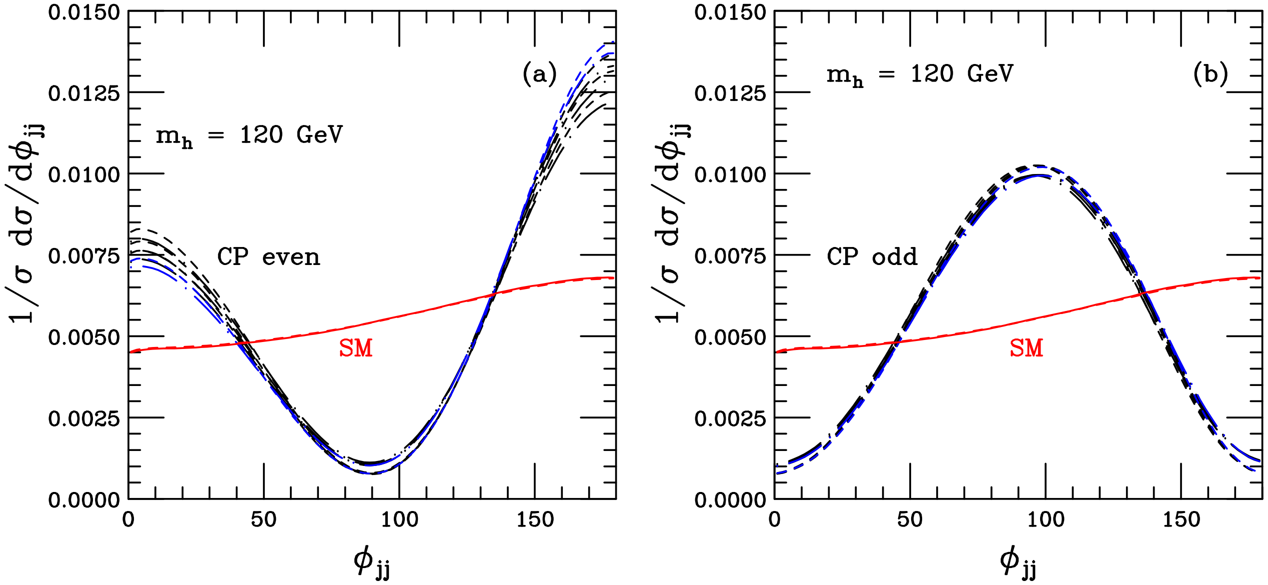

Form factor dependence is small.

The case: $a_2 = a_3$

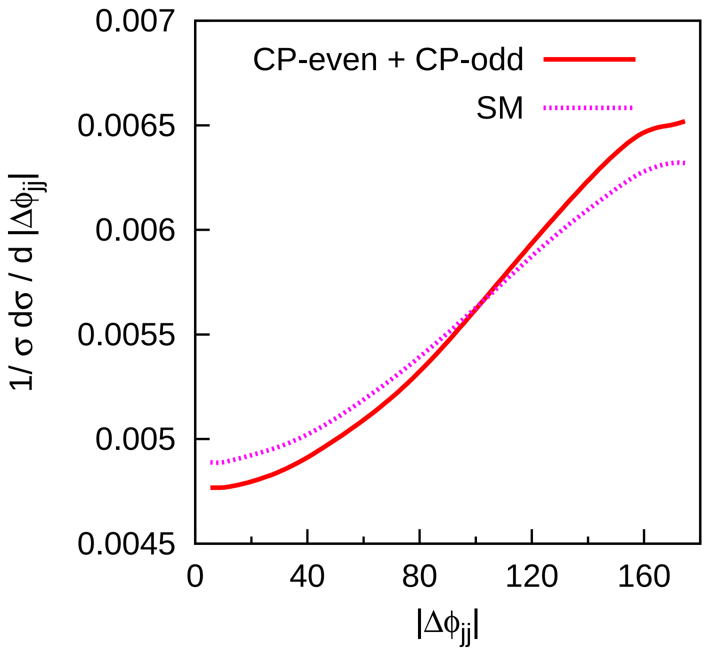

But, it doesn't work!

Redefinition of ϕ_{jj}

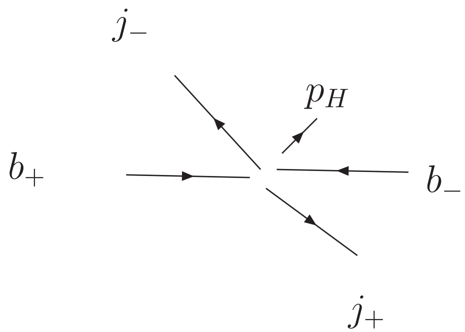

Within the last year [a], it has been suggested to define the azimuthal angle between j_+ and j_- as

$$\varepsilon_{\mu\nu\rho\sigma} b_+^\mu p_+^\nu b_-^\rho p_-^\sigma = 2 p_{T,1} p_{T,2} \sin(\phi_+ - \phi_-) = 2 p_{T,1} p_{T,2} \sin \Delta\phi_{jj}$$

- Invariant under $(b_+, p_+) \leftrightarrow (b_-, p_-)$
- Parity odd variable

[a] V. Hankele, G. Klamke, D. Zeppenfeld and T. Figy, Phys. Rev D74 (2006) 095001 hep-ph/0609075

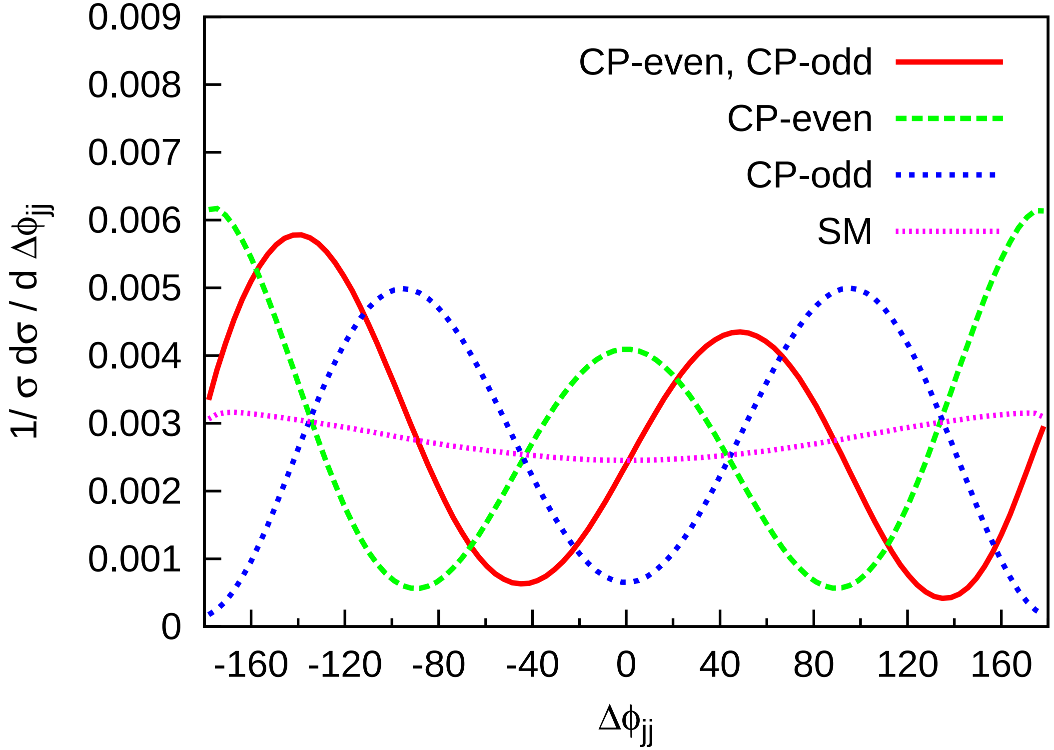

We're in business!

VBFNLO

- VBFNLO is a parton level Monte Carlo program for Vector Boson Fusion processes.
  - Vjj, $V = Z, W^{\pm}$: C. Oleari, D. Zeppenfeld. Phys. Rev. **D68** (2003) 073005
  - W^+W^-jj: B. Jager, C. Oleari, D. Zeppenfeld. JHEP **0607** (2006) 015
  - $ZZjj$: B. Jager, C. Oleari, D. Zeppenfeld. Phys. Rev. **D74** (2006) 1113006
  - Hjj : T. Figy, C. Oleari and D. Zeppenfeld, Phys. Rev. D **68**, 073005 (2003)
    T. Figy and D. Zeppenfeld, Phys. Lett. B **591**, 297 (2004)
    V. Hankele, G. Klamke, D. Zeppenfeld and T. Figy, Phys. Rev **D74** (2006) 095001

- Project members:

  M. Bähr, G. Bozzi, C. Englert, T. Figy, J. Germer, N. Greiner, K. Hackstein, V. Hankele, B. Jäger, G. Klämke, M. Kubocz, P. Konar, C. Oleari, M. Werner, M. Worek, D. Zeppenfeld

- The program can be downloaded from
  http://www-itp.physik.uni-karlsruhe.de/∼vbfnloweb/VBFNLO.

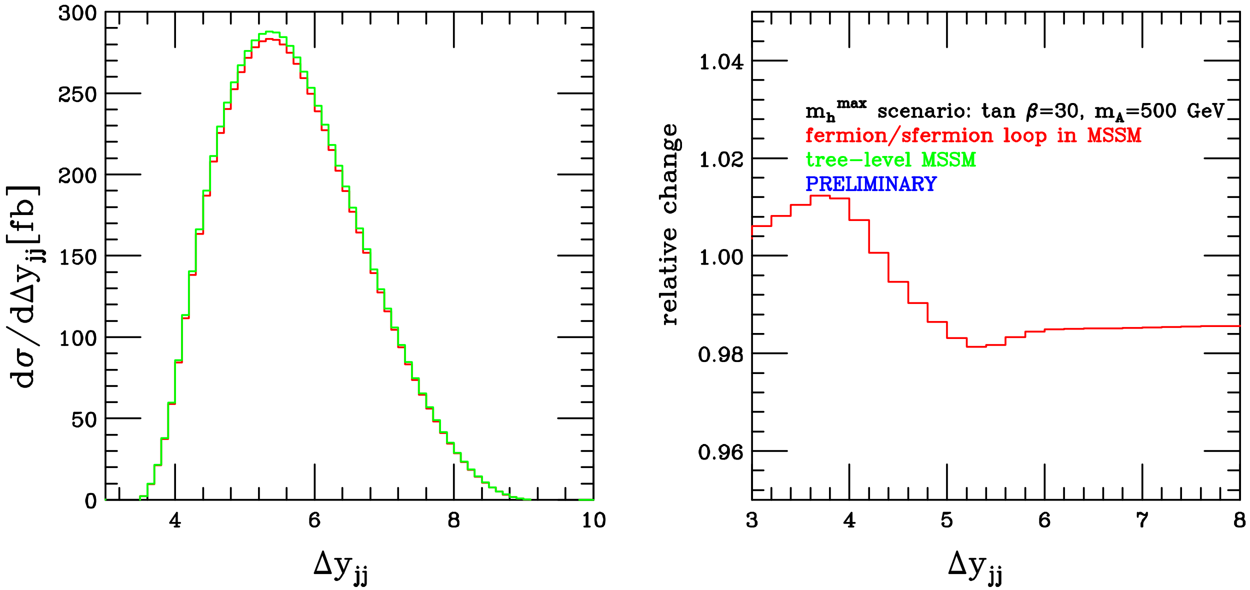

MSSM corrections to $h(H)VV$ couplings

A version of VBFNLO for MSSM light and heavy Higgs production has been developed by Sophy Palmer, Georg Weiglein, and TF that includes fermion/sfermion loop graphs that contribute to $H(h)VV$ couplings.

[MSSM results, differential cross section]

LHC, $\frac{d^2\sigma}{dp_{T,\text{jet}}\,d\eta_{\text{jet}}}$: MSSM – SM relative and absolute difference

relative difference in % :
contour lines ——

absolute difference :

- ● : 5 - 10 fb/GeV
- ▲ : 1 - 5 fb/GeV
- ■ : 0.5 - 1 fb/GeV
- ♦ : 0.1 - 0.5 fb/GeV

→ consider ratio :

$$R = \frac{\sigma\left(\begin{array}{c} p_T > 70\,\text{GeV} \\ |\eta| < 1.5 \end{array}\right)}{\sigma\left(\begin{array}{c} p_T \in [30, 50]\,\text{GeV} \\ |\eta| > 1.5 \end{array}\right)}$$

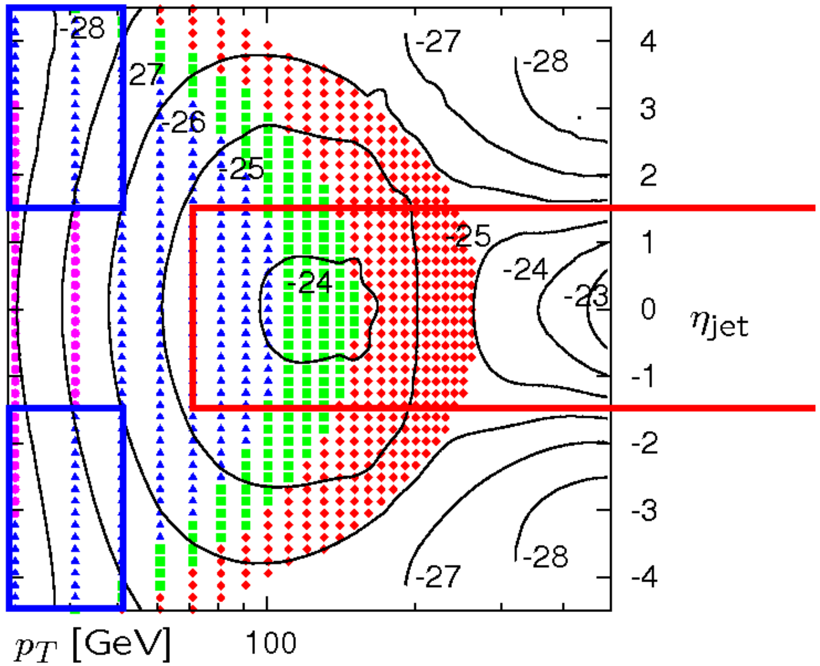

LHC, m_h-max scenario, $M_{\text{SUSY}} = 400$ GeV,
$m_A = 400$ GeV, $\tan\beta = 30$

Oliver Brein and Wolfgang Hollik, ”Distributions for MSSM Higgs boson + jet production at hadron collider”, aiXiv:0705.2744.

Central Jet Veto

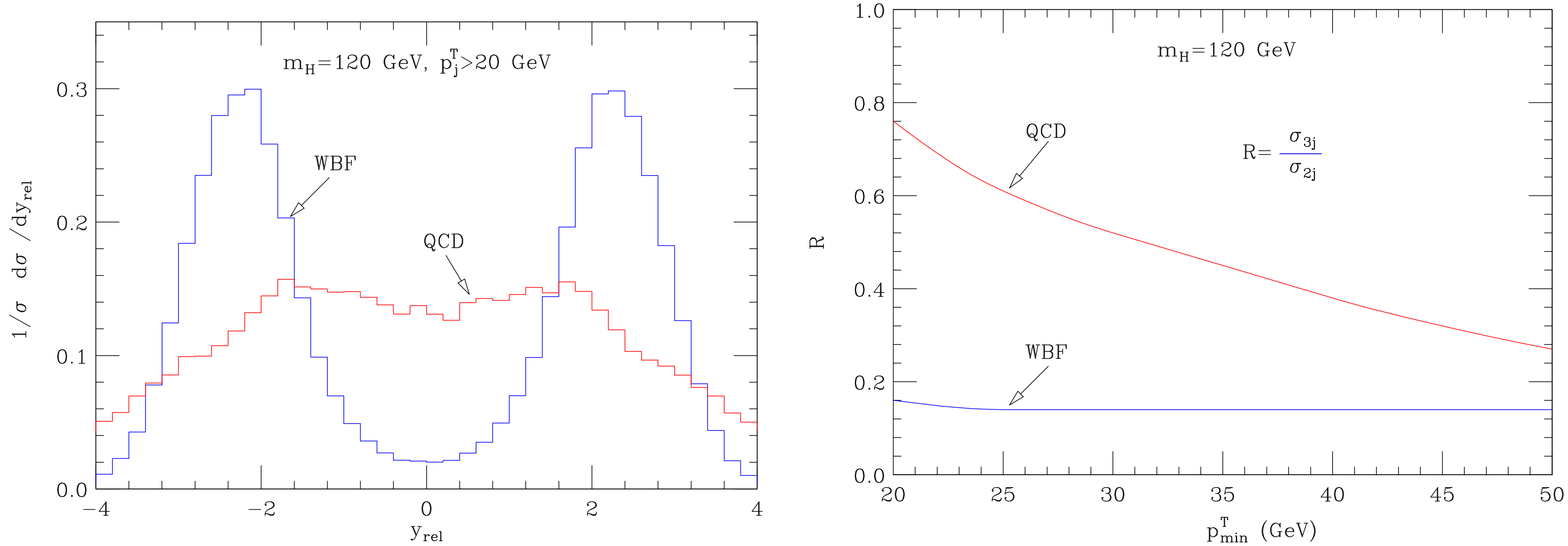

[JHEP 05 (2004) 064]

- A distinguishing feature of VBF is that at LO no color is exchanged in the t-channel.
- The central-jet veto is based on the different radiation pattern expected for VBF versus its major backgrounds [hep-ph/9412276, hep-ph/0012351]
- The central jet veto can be used to distinguish Higgs production via GF from VBF [hep-ph/0404013]

VBF signal and CJV

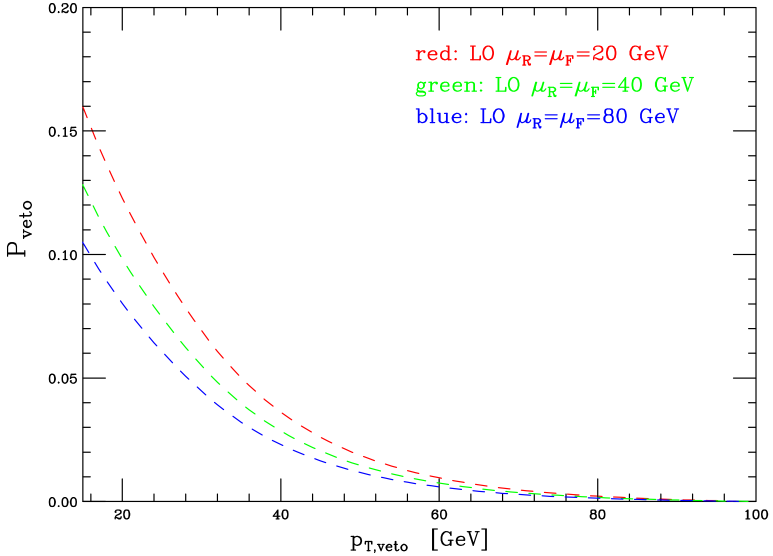

$$p_{Tj}^{veto} > p_{T,veto}, \quad \eta_j^{veto} \in (\eta_j^{\text{tag } 1}, \eta_j^{\text{tag } 2})$$

$$P_{\text{veto}} = \frac{1}{\sigma_2^{NLO}} \int_{p_{T,veto}}^{\infty} dp_{Tj}^{veto} \frac{d\sigma_3^{LO}}{dp_{Tj}^{veto}}$$

- Scale variation at LO for P_{veto}: $+33\%$ to -17% for $p_{T,veto} = 15$ GeV
- The uncertainty in P_{veto} feeds into the uncertainty of coupling measurements at the LHC: $\sigma(H) \times BR(H \to xx) = \frac{\sigma(H)^{SM}}{\Gamma_p^{SM}} \times \frac{\Gamma_p \Gamma_x}{\Gamma}$
- In order to constrain couplings more precisely, the NLO QCD corrections to $Hjjj$ are needed.

The NLO Calculation

The ingredients:

- Born: 3 final state partons + Higgs via VBF

$$\mathcal{M}_B = \delta_{i_2 i_b} t^{a_3}_{i_1 i_a} \Big[\mathcal{M}_{B,1a} :$$

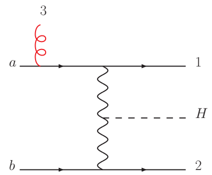

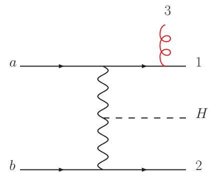

$$\Big]$$

$$+ \delta_{i_1 i_a} t^{a_3}_{i_2 i_b} \Big[\mathcal{M}_{B,2b} :$$

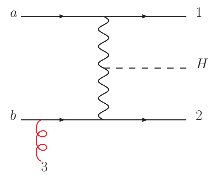

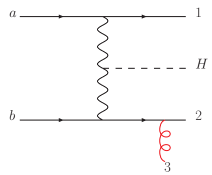

$$\Big]$$

- Virtual: Two gauge covariant subsets
  - Vertex + Propagator + Box
  - Pentagon + Hexagon
- Real: 4 final state partons + Higgs via VBF

T. M. Figy, Ph.D. Thesis, UMI-32-34582.
Paper is in preparation with Dieter Zeppenfeld and Vera Hankele of the ITP Karlsruhe.

Box+Vertex+Propagator corrections

$$\mathbf{Box} = \delta_{i_2 i_b} t^{a_3}_{i_1 i_a} \Big[\mathbf{Box(1a)} : $$

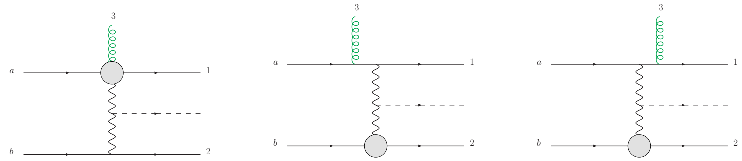

$$\Big]$$

$$+ \quad \delta_{i_1 i_a} t^{a_3}_{i_2 i_b} \Big[\mathbf{Box(2b)} : $$

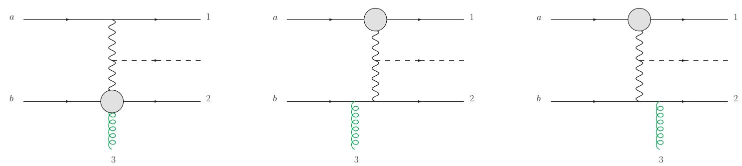

$$\Big]$$

Boxline Corrections

PV reduction used to reduce tensor loop integrals to scalar loop integrals.

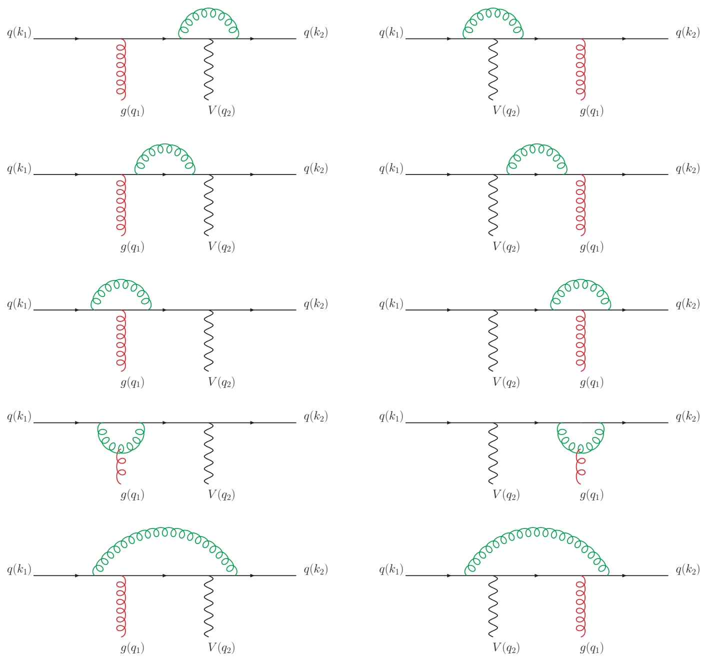

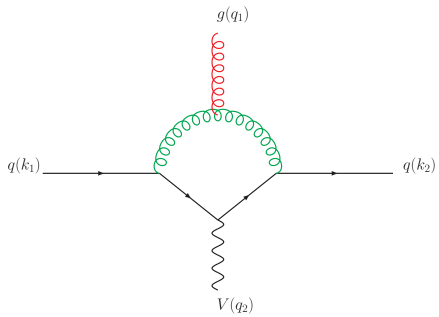

Hexagons and pentagons

These graphs contribute to the virtual corrections for $qQ \to qQgH$ and are color suppressed.

$$\mathbf{Hex}(\mathbf{1a}) + \mathbf{Pent}(\mathbf{1a}) = \left\{ \quad \right\}$$

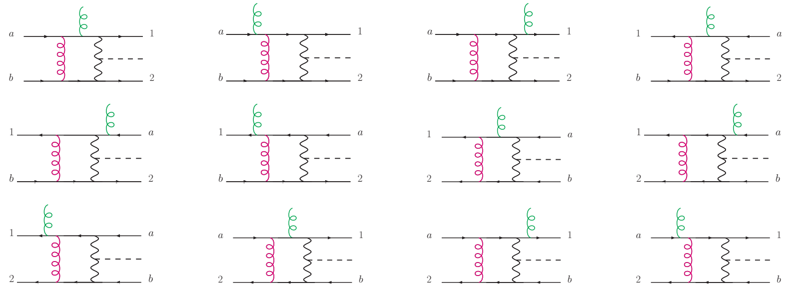

$$\begin{aligned} 2\ \mathrm{Re}\left[\mathcal{M}_V \mathcal{M}_B^*\right] &= d_F^2 C_F^2\ 2\ \mathrm{Re}\left[(\mathbf{Box}(\mathbf{1a}))\mathcal{M}_{B,1a}^*\right] \\ &+ d_F^2 C_F^2\ 2\ \mathrm{Re}\left[(\mathbf{Box}(\mathbf{2b}))\mathcal{M}_{B,2b}^*\right] \\ &+ \frac{d_F^2 C_F^2}{d_G}\ 2\ \mathrm{Re}\left[(\mathbf{Hex}(\mathbf{1a}) + \mathbf{Pent}(\mathbf{1a}))\mathcal{M}_{B,2b}^*\right] \\ &+ \frac{d_F^2 C_F^2}{d_G}\ 2\ \mathrm{Re}\left[(\mathbf{Hex}(\mathbf{2b}) + \mathbf{Pent}(\mathbf{2b}))\mathcal{M}_{B,1a}^*\right] \end{aligned}$$

To a first approximation, we may neglect the contribution of the hexagons and pentagons.

Real Corrections

$$\mathcal{M}_4(1_q, 2_Q, 3_g, 4_g, a_q, b_Q) = \left\{ \right.$$

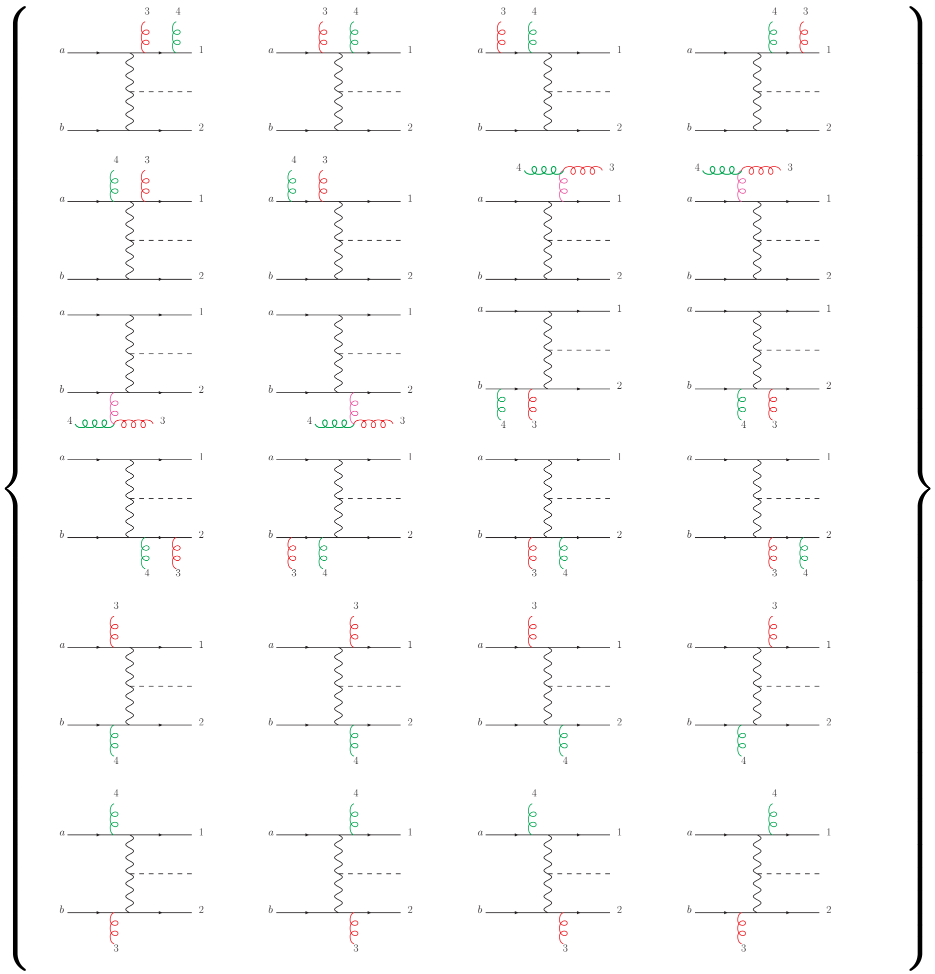

Treat Real Corrections Consistently!

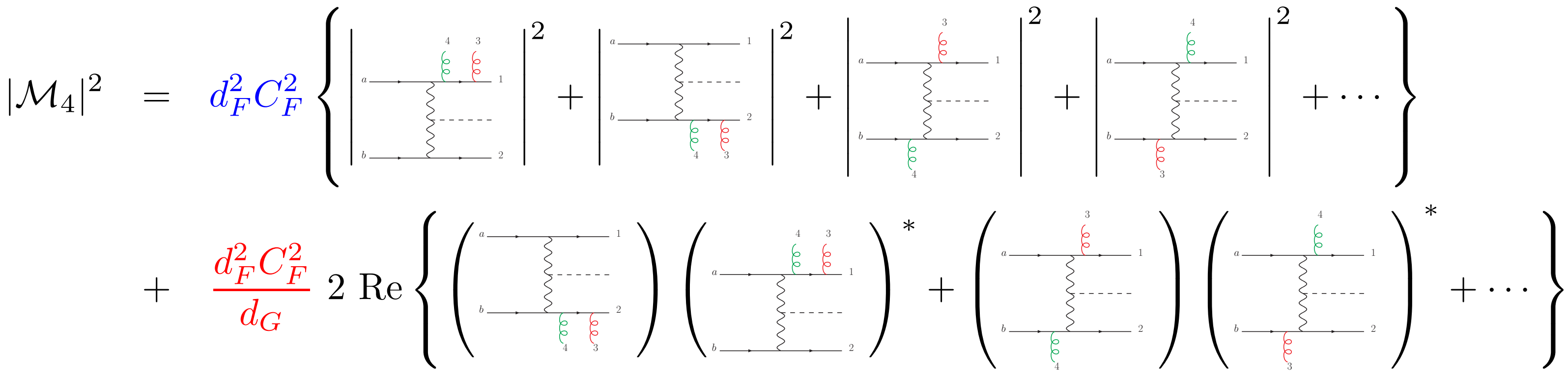

The term $\propto 1/d_G$ when integrated over PS gives rises to a soft divergence. This soft divergence is cancelled against the soft divergence arising from the hexagons and pentagons. For consistency, this term is also neglected.

Error Estimate on the Approximation

$\Delta\mathbf{NLO} \propto 2\,\mathrm{Re}\Bigg[\Bigg(\mathcal{M}_{B,1a}:$ 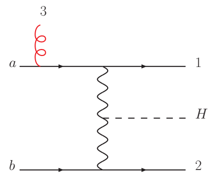

$+\ldots\Bigg)\Bigg(\mathcal{M}_{B,2b}:$ 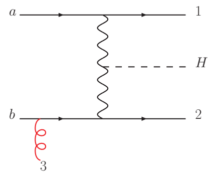

$+\ldots\Bigg)^*\Bigg]$

Left: $\Delta\sigma_3^{NLO}$ (solid) and σ_3^{LO} (dashes).

Right: $R(y_{\mathrm{rel}}) = \Delta\mathbf{NLO}/\mathbf{LO}$

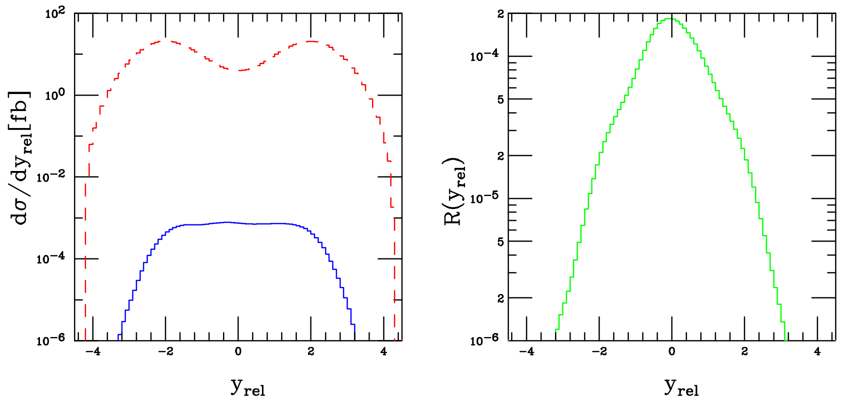

$\Delta\sigma_3^{NLO} \approx 10^{-3}$ fb for VBF cuts in the CJV region with $m_h = 120$ GeV.

NLO parton level Monte Carlo Program

- The dipole subtraction method of Catani and Seymour is used to regulate the IR divergences of the real emission corrections [hep-ph/9605323].
- Have introduced a cut, α, on the PS of the dipoles as a consistency check [hep-ph/0307268].
- Born amplitudes are calculated numerically using the helicity amplitude formalism.
- Real amplitudes were generated using MADGRAPH.
- Identical particle effects have been neglected.
- b-quarks have been included for neutral current processes.
- The Monte Carlo integration is performed with a modified form of VEGAS.
- CTEQ6M PDFs are used at NLO with $\alpha_s(M_Z) = 0.118$ while CTEQ6L1 PDFs are used at LO with $\alpha_s(M_Z) = 0.130$.
- SM parameters are computed using LO electroweak relations with M_Z, M_W, and G_F as inputs.
- Jets are reconstructed from final-state partons by the use of the k_T algorithm with $D = 0.8$.

VBF Cuts

- k_T algorithm: Require at least 3 hard jets with $p_{Tj} \geq 20$ GeV and $|y_j| \leq 4.5$.
- Tagging jets: 2 jets of $p_{Tj}^{\text{tag}} \geq 30$ GeV and $|y_j^{\text{tag}}| \leq 4.5$.
- Higgs decay products:

$$p_{T\ell} \geq 20 \text{ GeV}\,, \qquad |\eta_\ell| \leq 2.5\,, \qquad \triangle R_{j\ell} \geq 0.6 \tag{2}$$

$$y_{j,min}^{\text{tag}} + 0.6 < \eta_{\ell_{1,2}} < y_{j,max}^{\text{tag}} - 0.6. \tag{3}$$

- Rapidity gap and opposite detector hemispheres:

$$y_j^{\text{tag 1}} \cdot y_j^{\text{tag 2}} < 0 \tag{4}$$

$$\Delta y_{jj} = |y_j^{\text{tag 1}} - y_j^{\text{tag 2}}| > 4 \tag{5}$$

- Invariant mass of tagging jets:

$$m_{jj} = \left(p_j^{\text{tag 1}} + p_j^{\text{tag 2}}\right)^2 > 600 \text{ GeV} \tag{6}$$

NLO vs LO

Total Cross Section at the LHC

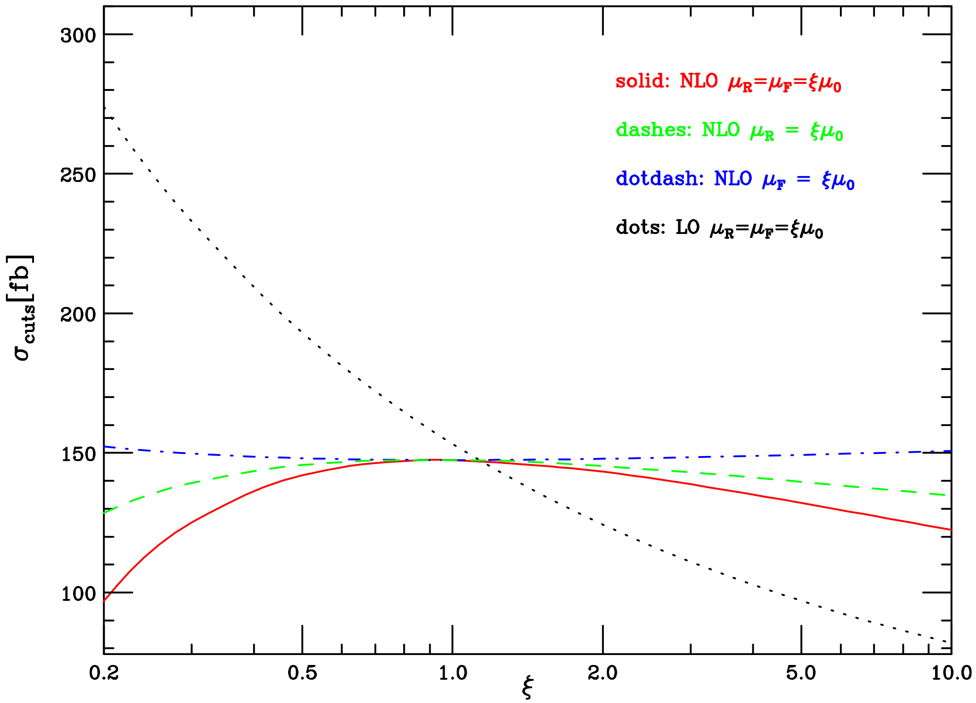

$\mu_0 = 40$ GeV

$\xi = 2^{\mp 1}$ scale variations:

- LO: +26% to −19%
- NLO: less than 5%

NLO vs LO

Tagging Jet Distributions

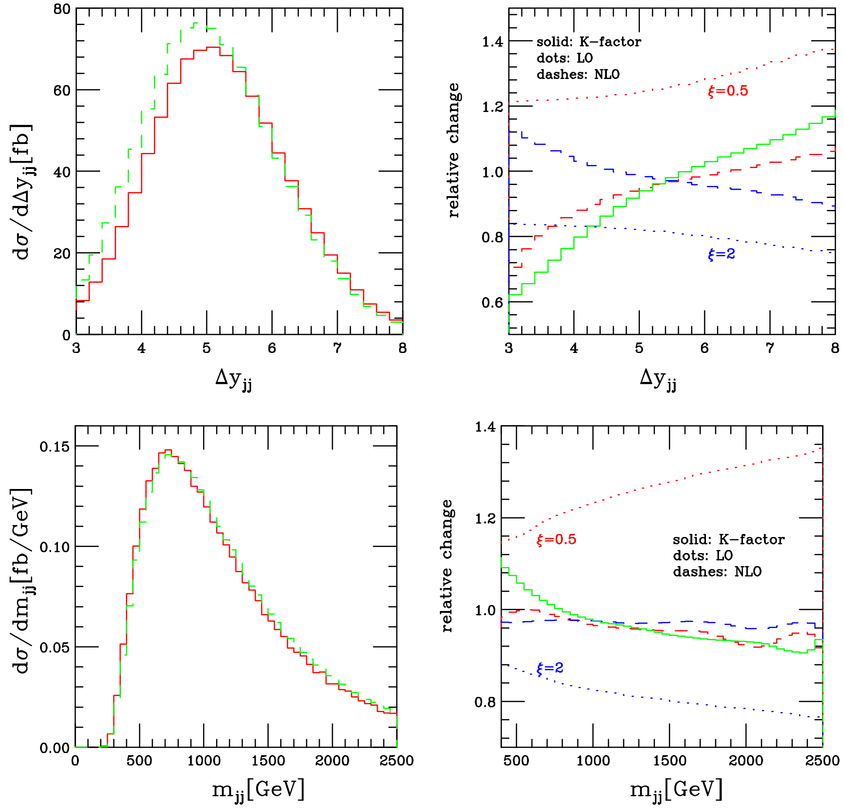

Left panel: NLO (solid) and LO (dashed).

Right panel:

$$K(x) = \frac{d\sigma_3^{NLO}(\mu_R = \mu_F = \xi\mu_0)/dx}{d\sigma_3^{LO}(\mu_R = \mu_F = \mu_0)/dx}$$

(solid) and

$$\text{relative change} = \frac{d\sigma_3(\mu_R = \mu_F = \xi\mu_0)/dx}{d\sigma_3(\mu_R = \mu_F = \mu_0)/dx}$$

at LO (dots) and NLO (dashes) for $\xi = 0.5$ and $\xi = 2$.

NLO vs LO

Veto Jet Distributions

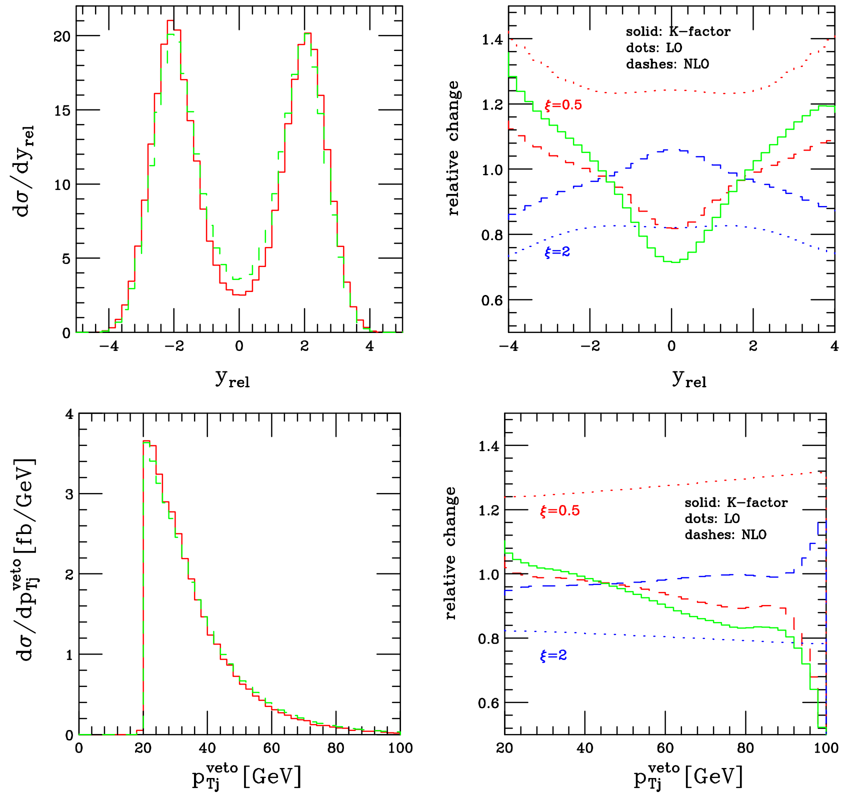

Central Jet Veto (CJV) cuts:

$$p_{Tj}^{\text{veto}} > 20 \text{ GeV}, \qquad y_j^{\text{veto}} \in (y_j^{\text{tag 1}}, y_j^{\text{tag 2}}). \quad (7)$$

$$y_{\text{rel}} = y_j^{\text{veto}} - (y_j^{\text{tag 1}} + y_j^{\text{tag 2}})/2$$

- Veto is slightly softer at NLO.
- $\xi = 2^{\mp 1}$ scale variations at y_{rel}=0:
  - LO: −27% to +42%
  - NLO: −20% to +7%
- Suppressed radiation in the vicinity of $y_{rel} = 0$.

NLO vs LO

VBF H+3 jets vs VBF H+2 jets

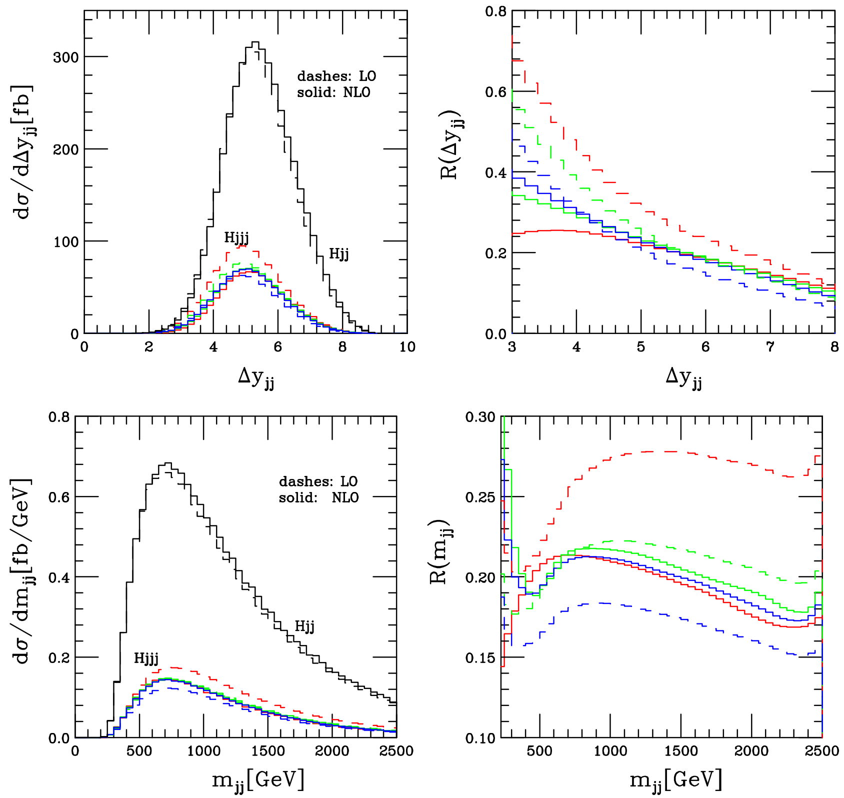

T. Figy, C. Oleari and D. Zeppenfeld, Phys. Rev. D **68**, 073005 (2003)

Top: VBF cuts, no $\Delta y_{jj} > 4$.

Bottom: VBF cuts, no $m_{jj} > 600$ GeV.

Right panel:

$$R(x) = \frac{d\sigma_3(\mu_R, \mu_F)/dx}{d\sigma_2^{NLO}(\mu_R = \mu_F = m_h)/dx}$$

Left panel:

- VBF H+3 jets at NLO (solid colored) and LO (dashes colored) with $\mu_R = \mu_F = 20, 40, 80$ GeV.
- VBF H+2 jets at NLO (solid black) and LO (dashes black).

NLO vs LO

VBF H+3 jets vs VBF H+2 jets in the CJV region

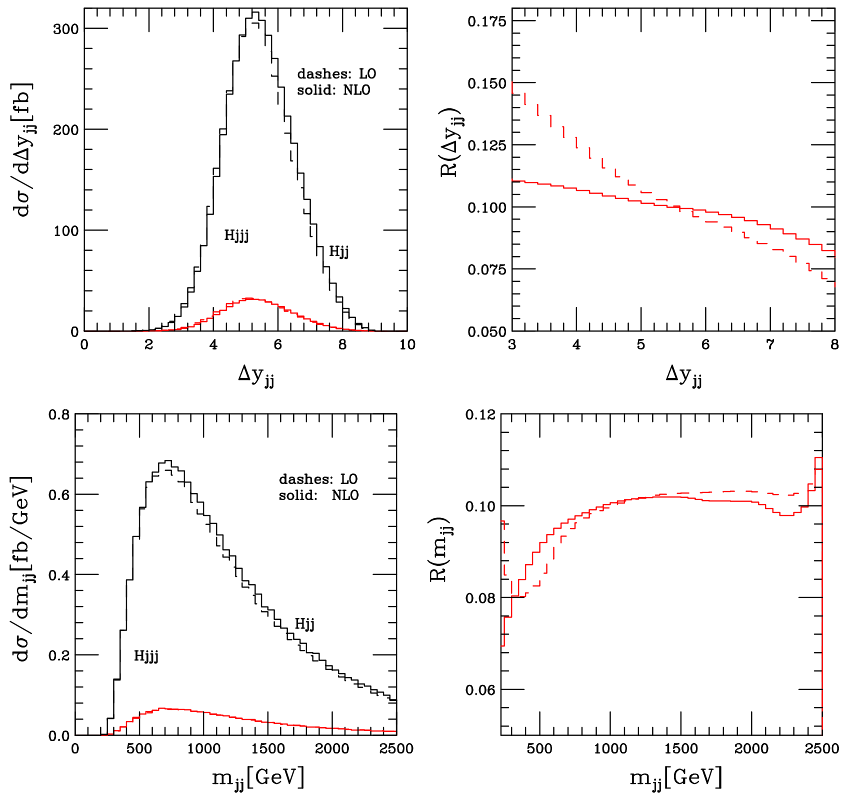

Top: CJV and VBF cuts, no $\Delta y_{jj} > 4$.
Bottom: CJV and VBF cuts, no $m_{jj} >$ 600 GeV.
Right panel:

$$R(x) = \frac{d\sigma_3(\mu_R, \mu_F)/dx}{d\sigma_2^{NLO}(\mu_R = \mu_F = m_h)/dx}$$

Left panel:

- VBF H+3 jets at NLO (solid) and LO (dashes) with $\mu_R = \mu_F = 40$ GeV.
- VBF H+2 jets at NLO (solid black) and LO (dashes black).

NLO vs LO

Veto Probability for the VBF Signal

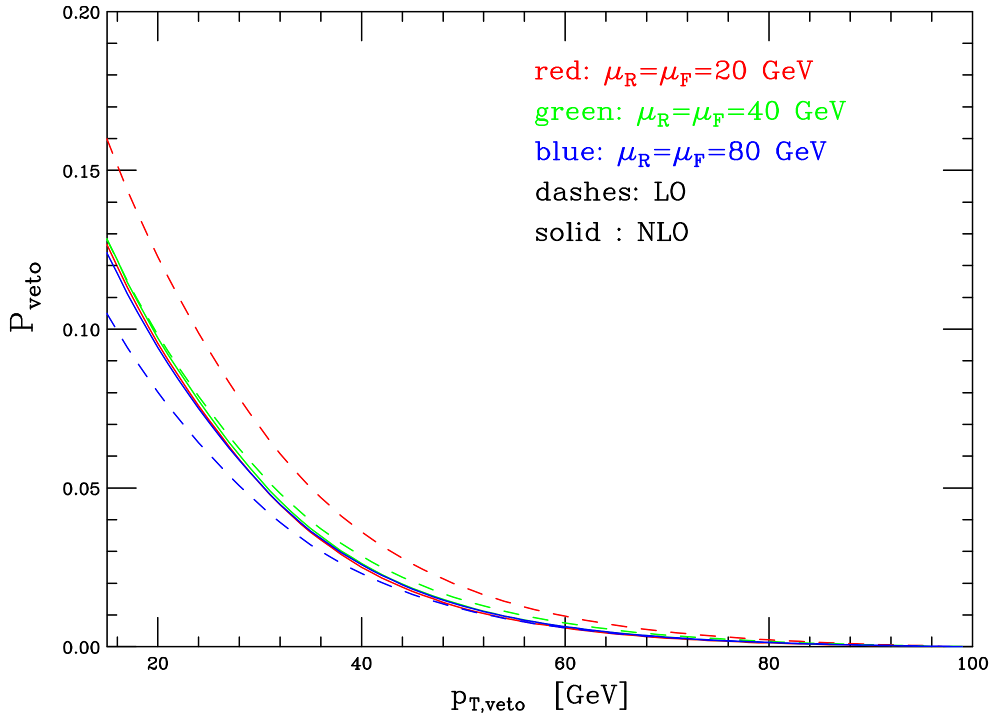

$$P_{\rm veto} = \frac{1}{\sigma_2^{NLO}} \int_{p_{T,veto}}^{\infty} dp_{Tj}^{veto} \frac{d\sigma_3}{dp_{Tj}^{veto}}$$

Scale variations, $p_{T,veto} = 15$ GeV:

- LO: +33% to −17%
- NLO: −1.4% to −3.4%

Final Remarks

- Various VBF processes have been calculated at NLO QCD are available: $Hjjj$,Hjj,Vjj,and $VVjj$.
- Scale dependence is reduced for the total cross section and distributions at NLO.
- K factors are phase space dependent. Shapes change at NLO!
- If we are too understand the mechanism for electroweak symmetry breaking, we need to consider higher-order effects.
- Theorists must not tell experimentalists they should include loops in calculations and not provide the the tools.

The Dipole Subtraction Method

Soft and collinear singularities of the real emission corrections are regulated by use of the dipole subtraction method of Catani and Seymour [hep-ph/9605323].

$$\begin{aligned}\sigma_{ab}^{NLO}(p,\bar{p}) &= \sigma_{ab}^{NLO\{4\}}(p,\bar{p}) + \sigma_{ab}^{NLO\{3\}}(p,\bar{p}) \\ &+ \int_0^1 dx[\hat{\sigma}_{ab}^{NLO\{3\}}(x,xp,\bar{p}) + \hat{\sigma}_{ab}^{NLO\{3\}}(x,p,x\bar{p})]\end{aligned}$$

$$\sigma_{ab}^{NLO\{4\}}(p,\bar{p}) = \int_4 [d\sigma_{ab}^{R}(p,\bar{p})_{\epsilon=0} - d\sigma_{ab}^{A}(p,\bar{p})_{\epsilon=0}]$$

$$\sigma_{ab}^{NLO\{3\}}(p,\bar{p}) = \int_3 [d\sigma_{ab}^{V}(p,\bar{p}) + d\sigma_{ab}^{B}(p,\bar{p}) \otimes \mathbf{I}]_{\epsilon=0}$$

$$\int_0^1 dx\hat{\sigma}_{ab}^{NLO\{3\}}(x,xp,\bar{p}) = \sum_{a'} \int_0^1 dx \int_3 \{d\sigma_{a'b}^{B}(xp,\bar{p}) \otimes [\mathbf{P}(x) + \mathbf{K}(x)]^{aa'}\}_{\epsilon=0}$$